

Optimal Number of Basis Functions in the MoM Solutions for Bodies of Revolution

Úrsula C. Resende, Fernando J. S. Moreira, Odilon M. C. Pereira-Filho, and João A. Vasconcelos*
Dept. Electronics Engineering, *Dept. Electric Engineering, Federal University of Minas Gerais
Av. Pres. Antonio Carlos 6627, Belo Horizonte, MG, CEP 31270-901, Brazil
resendeursula@gmail.com, fernandomoreira@ufmg.br, odilon@cpdee.ufmg.br, joao@cpdee.ufmg.br

Abstract— In this paper we present and investigate two new formulations, EMFIE (electric-magnetic field integral equation) and MEFIE (magnetic-electric field integral equation), for the solution of the electromagnetic scattering by dielectric and composites bodies of revolution. The new formulations are generated by the standard electric and magnetic field surfaces integral equations. EMFIE, MEFIE, EFIE, MFIE, CFIE, PMCWHT and Müller formulations numerically evaluated by the method of moments technique (MoM) are compared in the analysis of the scattering by bodies of revolution with small and large electric dimensions. Results are compared to Mie-series analytical solutions. It is shown that Müller formulation provides the most accurate solutions for homogeneous and layered dielectric bodies, and PMCWHT integral equation may provide the most accurate solutions for bodies composed of different homogeneous regions, independently of the relative permittivities. For conducting, dielectric and composites bodies of revolution it is investigated the minimum number of basis functions necessary to attain numerical convergence in the electromagnetic scattering analysis by CFIE and Müller (PMCWHT) formulations for conductor and dielectrics surfaces, respectively. Empirical formulas are derived for the optimal number of basis functions. These empirical formulas are used in the choice of the number of basis functions for an omnidirectional double reflector antenna analysis

Index Terms— Electric and magnetic field integral equations, electromagnetic scattering by bodies of revolution, Method of moments.

I. INTRODUCTION

Electromagnetic scattering from conducting, dielectric and composite bodies is an important and challenging problem in the field of computational electromagnetic. Analytical solutions are available for only very limited geometries. For bodies having an arbitrary shape, one has to resort to some approximate numerical technique. A variety of approaches have been developed to study this problem, which include the method of moments (MoM), the finite element method (FEM), and the finite-difference time-domain (FDTD) method. When the bodies are homogeneous, MoM is preferred because the problem can be formulated in terms of surface integrals over the conducting and dielectric surfaces [1]-[3]. In special for bodies of revolution (BOR) the problem is formulated in terms of integrals over generatrices [4]-[6]. For perfectly conducting (PEC) BOR the problem has been

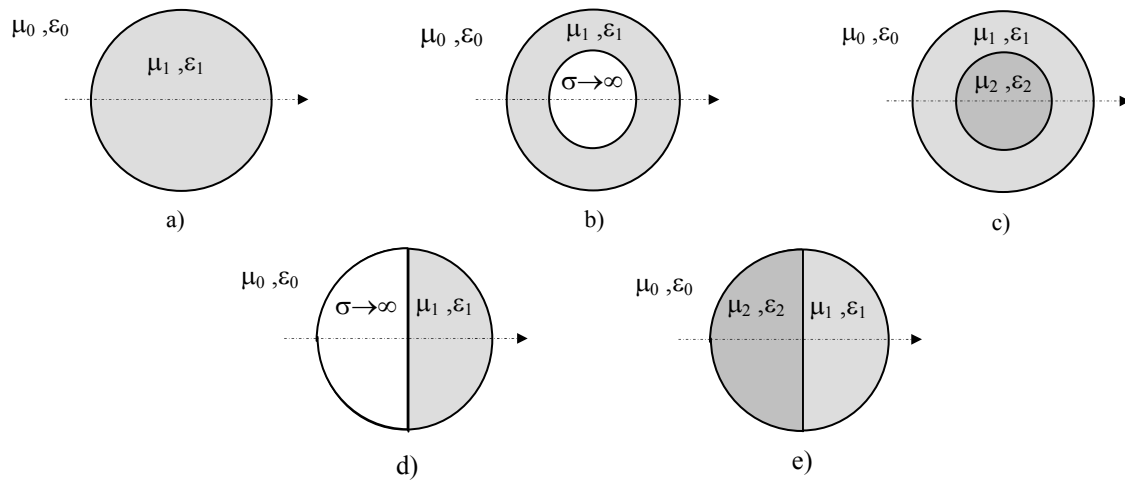


Fig. 1. Generic axially bodies of revolution. a) Dielectric body. b) Coated PEC body. c) Coated dielectric body. d) Body with dielectric and conducting regions e) Body with two dielectric regions.

exhaustively studied and the most accurate formulations are EFIE (electric field integral equation) and CFIE (combined field integral equation that is a linear combination of EFIE and MFIE - magnetic field integral equation) for open and closed conducting bodies, respectively [5]. For dielectric BOR, many combinations of EFIE and MFIE have been investigated [6]-[8]. Some of these are the EFIE, MFIE, CFIE, PMCHWT (solution proposed by Poggio, Miller, Chang, Harrington, Wu and Tsai), and Müller formulations [6]-[8]. Such solutions (or combinations of them) have also been used in the analysis of scattering by composite BOR as them shown in the Fig. 1 b) to e) [8]-[12].

The reported investigations are generally conducted for electrically small BOR (i.e., with dimensions of the order of the wavelength) [6]-[12]. In the present work we present and investigate two new formulations for solution of the electromagnetic scattering by dielectric and composites bodies, as those shown in Fig. 1. Plane-wave scattering from dielectric and composite spheres of different electrical sizes and different relative permittivity (ϵ_r) values are adopted as study cases. The study shows that the new formulations are accurate for scattering analysis by different types of BOR. We also conduct an investigation of the performance of several formulations in the analysis of the scattering by dielectric and composite BOR with large electric dimensions (e.g., spheres with radii up to $25\lambda_0$) and for a wide range of relative dielectric permittivities ($1 < \epsilon_r < 100$). The BOR geometries to be considered are the homogeneous dielectric spheres, PEC spheres coated by a dielectric substrate and sphere with two homogeneous hemispheres. Analytical Mie-series solutions are available [13] and used as references in the accuracy analysis of different integral equations solutions.

In this work we adopt the versatile triangular basis functions (TBF) to represent the current spatial variation along the BOR generatrix. Closed conducting and dielectric surfaces are analyzed by CFIE and Müller (PMCHWT) formulation, respectively. For several different dielectric, conducting and composite spheres, we obtain the minimum number of segments (i.e., basis functions) necessary to attain a desired accuracy for the current representation. The study leads to empirical formulas that

provide the optimal (minimum) number of segments (ONS) in terms of the sphere relative permittivity (for dielectrics) and electrical radius. Such formulas are used in the choice of the number of basis functions for omnidirectional double-reflector antenna analysis and it is demonstrated that such empirical formulas are able to provide the necessary ONS for analysis of more complex BOR.

II. PROBLEM FORMULATION

For a homogeneous body, as that shown in Fig. 1 a), with permittivity ϵ_1 and permeability μ_1 , immersed in an infinite and homogeneous medium with permittivity ϵ_0 and permeability μ_0 , the equivalence principle can be applied to establish a set of four integral equations (the EFIE and MFIE, for fields inside and outside the body) to solve for the electric (\mathbf{E}) and magnetic (\mathbf{H}) fields in terms of equivalent electric (\mathbf{J}) and magnetic (\mathbf{M}) surface currents [6]. Assuming that the sources of the incident field (\mathbf{E}^{inc} , \mathbf{H}^{inc}) are outside the body, the integral equations for the tangential field components can be represented as [6]:

$$[\eta_0 \mathbf{L}_0(\mathbf{J}) + \mathbf{K}_0(\mathbf{M})]_{\text{tan}} = \mathbf{E}_{\text{tan}}^{\text{inc}} \quad (1)$$

$$[\mathbf{L}_0(\mathbf{M}) - \eta_0 \mathbf{K}_0(\mathbf{J})]_{\text{tan}} = \mathbf{H}_{\text{tan}}^{\text{inc}}, \quad (2)$$

$$[\eta_1 \mathbf{L}_1(\mathbf{J}) + \mathbf{K}_1(\mathbf{M})]_{\text{tan}} = 0, \quad (3)$$

$$[\mathbf{L}_1(\mathbf{M}) - \eta_1 \mathbf{K}_1(\mathbf{J})]_{\text{tan}} = 0, \quad (4)$$

where the index i represents the interior ($i = 1$) and exterior ($i = 0$) regions, and L_i and K_i are

$$\mathbf{L}_i(\mathbf{X}) = \frac{j}{k_i} \int_{k_i}^j \int_{s'} [k_i^2 \mathbf{X}(\mathbf{r}') G_i(\mathbf{r}, \mathbf{r}') - \nabla' \mathbf{X}(\mathbf{r}') \nabla' G_i(\mathbf{r}, \mathbf{r}')] ds', \quad (5)$$

$$\mathbf{K}_i(\mathbf{X}) = \nu_i \hat{n} \times \frac{\mathbf{X}(\mathbf{r})}{2} + \int_{s'} [\mathbf{X}(\mathbf{r}') \times \nabla' G_i(\mathbf{r}, \mathbf{r}')] ds', \quad (6)$$

where S denotes the surface of the BOR, \hat{n} is the unit vector normal to the BOR surface, \mathbf{X} is either the equivalent electric or magnetic current on S , ν_i is a constant that values 1 if the field point resides on the outer surface and values -1 if the field point resides on the inner surface, and

$$G_i(\mathbf{r}, \mathbf{r}') = \frac{e^{-jk_i |\mathbf{r}, \mathbf{r}'|}}{4\pi |\mathbf{r}, \mathbf{r}'|} \quad (7)$$

is the free space Green's function of region i [6].

III. INTEGRAL EQUATION FORMULATIONS

In (1)-(4) there are four integral equations and two unknowns (\mathbf{J} and \mathbf{M}). So, it is possible to develop a number of different combinations among (1)-(4) to solve for \mathbf{J} and \mathbf{M} .

A. PEC Bodies

For PEC bodies, the EFIE (1), with $\mathbf{M} = 0$, is the best choice for open shells [5]. For closed-surface

bodies, the CFIE avoids spurious resonances and, consequently, provides stable numerical solutions [5]. The CFIE is a linear combination of (1) and (2) with $\mathbf{M} = 0$:

$$\alpha' \text{EFIE}_0 + \beta' \text{MFIE}_0, \quad (8)$$

where EFIE_0 and MFIE_0 represent (1) and (2), respectively, and a α' and β' are the linear-combination weights [5].

B. Homogeneous Dielectric Bodies

For dielectric bodies, (1)-(4) can be combined in many different ways to yield two integral equations suited to determine \mathbf{J} and \mathbf{M} [6]. The commonly adopted combinations are:

- i) EFIE: using the EFIE's (1) and (3).
- ii) MFIE: using the MFIE's (2) and (4).
- iii) CFIE: combining (1) with (2) and (3) with (4) to obtain two new integral equations, (8) and [6]:

$$\alpha' \text{EFIE}_1 + \beta' \text{MFIE}_1, \quad (9)$$

where EFIE_1 and MFIE_1 represent (3) and (4), respectively.

Another way to reduce the number of equations is to combine the (1)-(4) in the following way

$$\text{EFIE}_0 + \alpha \text{EFIE}_1, \quad (10)$$

$$\text{MFIE}_0 + \beta \text{MFIE}_1, \quad (11)$$

where linear-combination weights α and β are

- iv) PMCHWT: $\alpha = \beta = -1$ [6]-[9].
- v) Müller: $\alpha = \epsilon_1/\epsilon_0$ and $\beta = \mu_1/\mu_0$ [6]-[9].

Using two different combinations among (1)-(4) the new formulations are:

- vi) EMFIE (electric-magnetic field integral equation): using EFIE_0 , (1), and MFIE_1 , (4).
- vii) MEFIE (magnetic-electric field integral equation): using MFIE_0 , (2), and EFIE_1 , (3).

C. Composite bodies

For composite bodies (i.e., bodies composed of PEC and homogeneous dielectric regions), PEC surfaces are analyzed by (8), with $\beta' = 0$ for open PEC shells, while the interfaces between dielectric regions can, in principle, be treated by any combination cited in Sect. III-B [6]-[9].

IV. MOM SOLUTION

The scattering from the geometries depicted in Fig. 1 can be analyzed by the integral equations cited in Sects. II and III, which are evaluated by the well-known MoM technique, appropriately suited to the analysis of BOR [3]-[6]. For that, the surface currents \mathbf{J} and \mathbf{M} must be described in terms of basis functions along the BOR generatrix, with azimuthal variations described in terms of Fourier harmonics. In order to improve the accuracy and convergence of the MoM solution, the basis functions must be adequately represented. In this work, that is accomplished by employing the versatile triangular basis functions (TBF) to represent the spatial variations along the BOR generatrix

[4]. The TBF is defined over two consecutive segments that describe the BOR generatrix, as shown in Fig. 2. The unknown currents \mathbf{J} and \mathbf{M} are described as:

$$\mathbf{X}(\mathbf{r}') = \sum_{n=-\infty}^{\infty} \left[\sum_{j=1}^{N_t} I_{jn}^{X_t} \frac{T_j^t(t')}{\rho'} \hat{t}' + \sum_{j=1}^{N_\phi} I_{jn}^{X_\phi} \frac{T_j^\phi(t')}{\rho'} \hat{\Phi}' \right] e^{jn\phi'}, \quad (12)$$

where \mathbf{X} represents either \mathbf{J} or \mathbf{M} , \hat{t}' and $\hat{\Phi}'$ are unit directions tangential to the surface S at the source point \mathbf{r}' , $T_j^t(t')$ and $T_j^\phi(\phi')$ are TBF's (see Fig. 2), $I_{jn}^{X_\phi}$ and $I_{jn}^{X_t}$ are the unknowns coefficients of \mathbf{X} and N_t and N_ϕ are the number of TBF in \hat{t}' and $\hat{\Phi}'$ directions, respectively. In (12), the term $e^{jn\phi}$ corresponds to the Fourier expansion in ϕ and the division by ρ' prevents singularity problems at the symmetry axis.

The integral equations were evaluated by the MoM (weight functions were choose by Galerkin's technique). All integrals appearing in the computation of the Z-matrix terms were evaluated using Legendre-Gauss quadrature. However, the integral equations have singularities whenever observation is made upon the source location. In the singular regions adequate cautions are considered at the numerical evaluation of integrals. In this paper the singularities are removed using singularity extraction technique [4]. In this technique singular kernel is extracted and solved in closed form.

V. STUDY CASES

In this work numerical results are compared with analytical data, Mie-series [13], using the following mean relative error

$$E_{MR} (\%) = \frac{E_{Rt} + E_{R\phi} + E_{RM_t} + E_{RM_\phi}}{4}, \quad (13)$$

where the mean relative error E_{MR} takes into account the mean relative errors of the tangential \hat{t}' and $\hat{\Phi}'$ components of \mathbf{J} and \mathbf{M} (E_{RX}), according to:

$$E_{RX} (\%) = 100 \frac{\max \left| \left| \mathbf{X}^{MoM} \right| - \left| \mathbf{X}^{Mie} \right| \right|}{\max \left| \mathbf{X}^{Mie} \right|} \quad (14)$$

where \mathbf{X}^{MoM} and \mathbf{X}^{Mie} are the numerical, MoM, and the analytical, Mie-series, solutions elements, respectively.

A. New formulations results

For a dielectric sphere, as that shown in Fig. 1 a), with radius $R = 0.5 \lambda_0$, where λ_0 is the wavelength in vacuum (which surrounds the spheres), and $\epsilon_r = 25$, computed electric and magnetic currents in \hat{t}' direction are plotted in Fig. 3 as functions of surface coordinate $S(\lambda_0)$, which value 0 on the front of the sphere to $2\pi R$ on the back of the sphere. In this case 71 TBF were used to represent the current

spatial variation along of the BOR generatrix. The agreement between numerical and

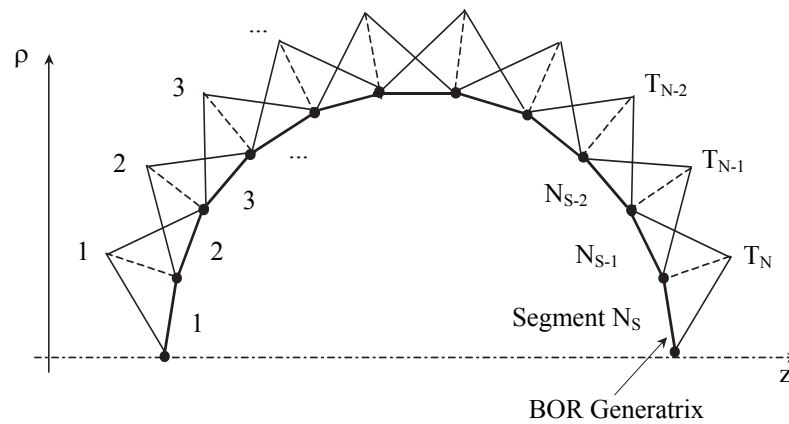


Fig. 2. Triangular basis functions (TBF).

analytical results is excellent and E_{MR} , is equal to 0.88 % and 0.99 % for EMFIE and MEFIE, respectively, and equal to 0.825 % for classical Müller formulation. For a dielectric sphere with $R = 10 \lambda_0$ and $\epsilon_r = 10$, computed currents in \hat{t}' direction as functions of $S(\lambda_0)$ are presented in Fig. 4. In this case 785 TBF were used to represent the current spatial variation. The agreement between numerical and analytical results is excellent and E_{MR} , is equal to 0.592 % and 1.05 % for EMFIE and MEFIE, respectively, and equal to 0.80 % for classical Müller formulation.

Next we studied the scattering by conducting coated spheres as shown in Figs. 1 b) and 5. In the first case $a = 5 \lambda_0$, $b = 0.55 \lambda_0$, $\epsilon_r = 10$ and 79 TBF were used to represent the current spatial variation in each BOR generatrix. Fig. 6 shows computed electric and magnetic currents in \hat{t}' direction in the dielectric external surface as functions of $S(\lambda_0)$. The agreement between numerical and analytical results is excellent and E_{MR} is equal to 0.56 % and 0.58 % for EMFIE and MEFIE, respectively, and equal to 0.589 % for classical Müller formulation. For $a = 5.0 \lambda_0$, $b = 5.5 \lambda_0$ and $\epsilon_r = 10$ the computed electric and magnetic currents in \hat{t}' direction in the dielectric external surface as functions of $S(\lambda_0)$ are presented in Fig. 7. In this case 471 TBF were used to represent the current spatial variation in each BOR generatrix. The agreement between numerical and analytical results is excellent and E_{MR} , is equal to 0.44 % and 1.25 % for EMFIE and MEFIE, respectively, and equal to 0.478 % for classical Müller formulation.

In the Fig. 5 considering internal sphere dielectric, $a = 5.0 \lambda_0$ with $\epsilon_r = 9$ and $b = 5.5 \lambda_0$ with $\epsilon_r = 10$, the computed electric and magnetic currents in \hat{t}' direction in the dielectric external surface as functions of $S(\lambda_0)$ are presented in Fig. 8. In this case 550 TBF were used to represent the current spatial variation. The agreement between numerical and analytical results is excellent and E_{MR} , is equal to 0.98 % and 0.81 % for EMFIE and MEFIE, respectively, and equal to 0.256 % for classical Müller formulation.

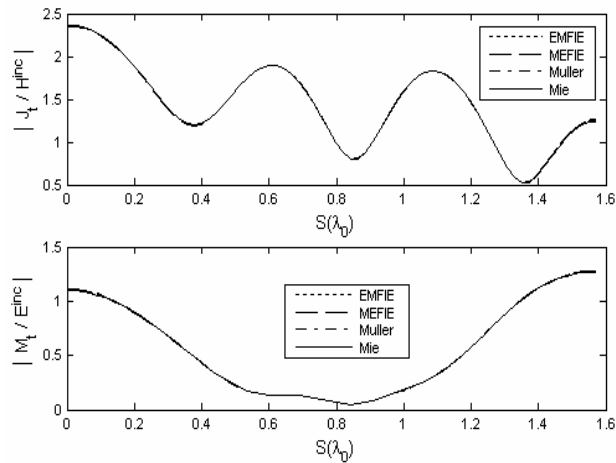


Fig. 3. Dielectric sphere $R = 0.5 \lambda_0$, $\epsilon_r = 25$. a) Electric current J_t . b) Magnetic current M_t .

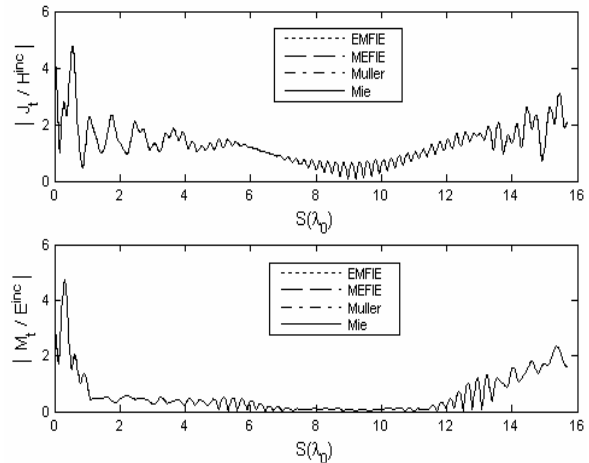


Fig. 4. Dielectric sphere $R = 10 \lambda_0$, $\epsilon_r = 10$. a) Electric current J_t . b) Magnetic current M_t .

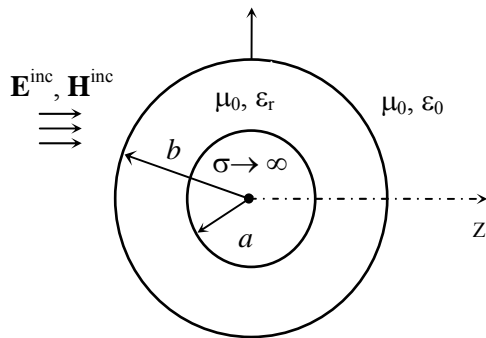


Fig. 5. Coated sphere.

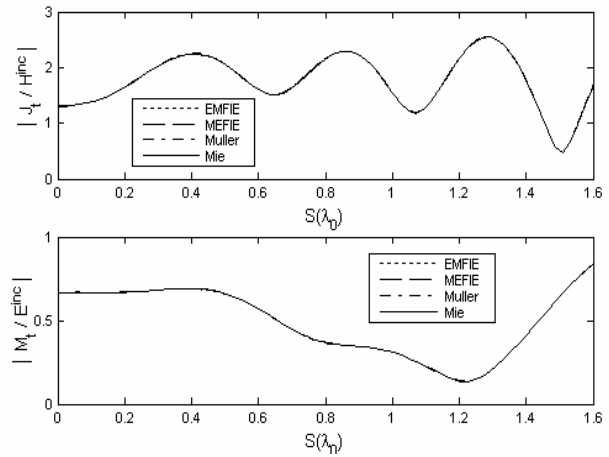


Fig. 6. PEC coated sphere $a = 0.5 \lambda_0$, $b = 0.55 \lambda_0$ and $\epsilon_r = 10$. a) Electric current J_t . b) Magnetic current M_t .

For a bisected sphere, as that shown in Figs. 1 e) and 9, with $a = 20 \lambda_0$, $\epsilon_{r1} = 4$ and $\epsilon_{r2} = 8$ the external electric and magnetic surface current in \hat{t}' direction as functions of $S(\lambda_0)$ are presented in Fig. 10. In this case 942 TBF were used to represent the external surface current spatial variation along the external BOR generatrix. The agreement between numerical solutions obtained by EMFIE, MEFIE and classical PMCHWT formulations is not so good as in the previous tests, but acceptable [10],[14] and [15]. The E_{MR} in relation to classical PMCHWT formulation is equal to 6.21 % and 3.12 % for EMFIE and MEFIE, respectively. Finally, Fig. 11 shows computed external surface electric and magnetic currents in \hat{t}' direction as functions of $S(\lambda_0)$ for bisected sphere shown in the Fig. 9, with $a = 20 \lambda_0$ and $\epsilon_{r1} = \epsilon_{r2} = 4$. The homogeneous sphere results are obtained from Mie series. Since both scatters are physically identical, this case provides an excellent test of the accuracy. In this case 942 TBF were used to represent the external surface current spatial variation. The agreement between numerical results is excellent and E_{MR} is equal to 0.602 % and 1.122 % for EMFIE and MEFIE,

respectively, and equal to 0.478 % for classical PMCHWT formulation.

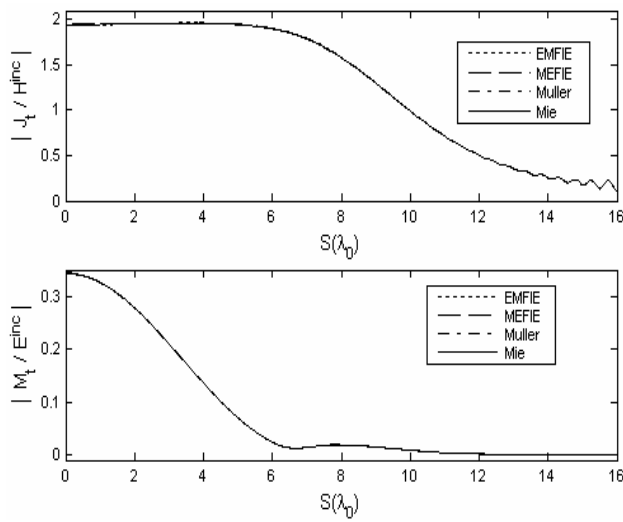


Fig. 7. PEC coated sphere $a = 5.0 \lambda_0$, $b = 5.5 \lambda_0$ and $\epsilon_r = 10$. a) Electric current J_t . b) Magnetic current M_t .

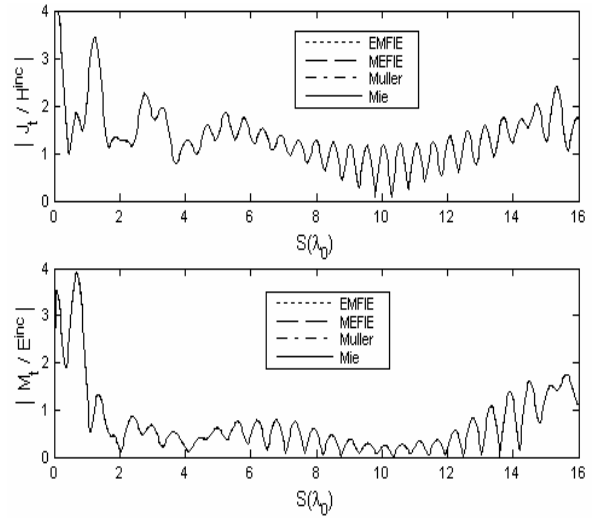


Fig. 8. Dielectric coated sphere $a = 5.0 \lambda_0$ with $\epsilon_r = 9$ and $b = 5.5 \lambda_0$ with $\epsilon_r = 10$. a) Electric current J_t . b) Magnetic current M_t .

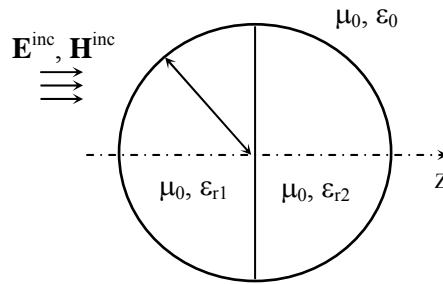


Fig. 9. Bisected sphere.

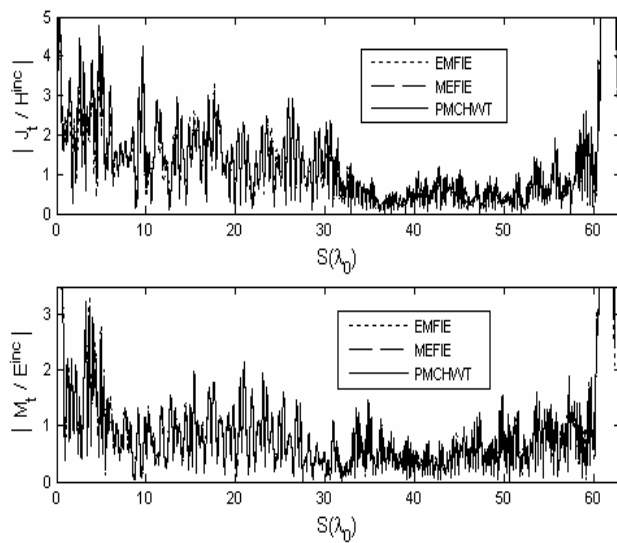


Fig. 10. Electric and magnetic current in external surface of bisected Sphere ($a = 20 \lambda_0$, $\epsilon_{r1} = 4$ and $\epsilon_{r2} = 8$). a) Electric current J_t . b) Magnetic current M_t .

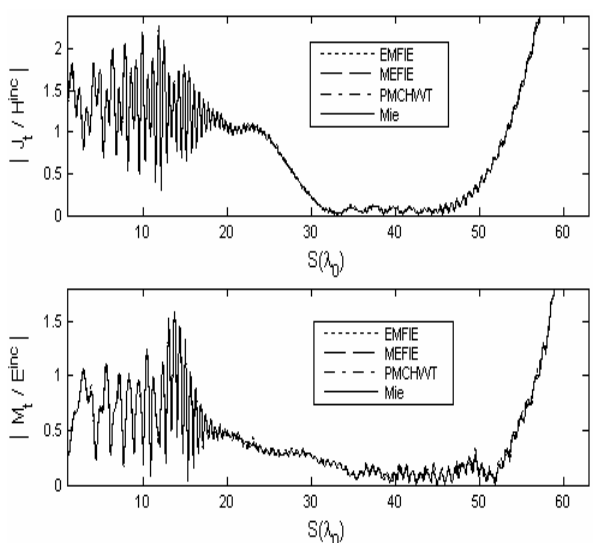


Fig. 11. Electric and magnetic current in external surface of bisected Sphere ($a = 20 \lambda_0$ and $\epsilon_{r1} = \epsilon_{r2} = 4$). a) Electric current J_t . b) Magnetic current M_t .

B. Comparison between formulations

In this section we investigate the performance of EFIE, MFIE, CFIE, PMCHWT, Müller, EMFIE and MEFIE formulations in the analysis of the scattering by dielectric and composite BOR with large electric dimensions (i.e., spheres with radii up to $25\lambda_0$) and for a wide range of relative dielectric permittivities ($1 < \epsilon_r < 100$). Initially, estimates of E_{MR} were obtained for a homogeneous dielectric sphere and some of the results are summarized in the Table I. For each line of Table I, all MoM solutions were obtained with the same number of TBF's, in order to ensure proper comparisons. As one can inspect from Table I the most accurate solution is generally that based on Müller formulation, particularly for smaller values of ϵ_r , as already observed in Sect. V-A and in [6] and [7] (for objects with smaller electrical dimensions).

TABLE I - MEAN RELATIVE ERROR (E_{MR}) FOR DIFFERENT DIELECTRIC SPHERES

Sphere radius	ϵ_r	E_{MR} (%)						
		Müller	PMCHWT	EFIE	MFIE	CFIE	EMFIE	MEFIE
$0.5 \lambda_0$	2	0.80	1.93	1.25	1.12	1.24	1.07	1.17
	10	0.88	4.29	3.59	0.76	0.76	0.90	11.25
	25	0.82	1.37	0.88	0.9	0.88	0.88	0.99
	50	1.32	4.55	2.4	1.61	2.41	3.31	4.52
	100	0.99	2.38	1.96	1.53	1.34	1.09	1.97
$2 \lambda_0$	2	0.99	2.53	1.80	1.52	1.18	1.16	1.45
	10	0.62	0.77	1.4	0.68	3.09	1.26	0.86
	25	1.36	50.1	24.6	4.04	2.46	1.77	5.09
	50	0.84	1.71	1.08	1.33	1.32	1.46	1.91
	100	1.09	4.56	2.12	1.91	17.2	1.21	7.79
$5 \lambda_0$	2	1.01	4.25	3.52	2.05	1.67	1.49	2.40
	10	1.07	3.35	2.27	2.2	2.13	1.39	54.29
	25	1.08	2.23	1.55	2.38	9.62	1.27	2.79
	50	1.86	1.59	0.88	1.54	0.9	1.52	1.99
	100	1.74	2.92	6.88	2.98	11.68	1.76	5.14
$10 \lambda_0$	2	0.99	2.74	2.28	1.62	2.44	1.70	1.88
	10	0.80	1.17	0.84	0.59	1.27	0.59	1.05
	25	13.36	17.92	15.88	17.34	16.71	14.69	18.46
	50	1.12	1.42	1.28	7.72	1.25	1.05	2.21
	100	1.75	2.92	-	-	-	-	-
$25 \lambda_0$	2	1.77	2.71	2.48	2.59	2.55	2.58	2.26
	10	1.49	2.90	3.61	0.96	1.54	-	-
	25	6.06	7.38	19.8	4.58	10.9	-	-

For PEC spheres coated with a dielectric substrate, as that shown in Fig. 1 b), E_{MR} obtained by EFIE, MFIE, CFIE, PMCHWT, Müller, EMFIE and MEFIE solutions for several radii and relative permittivities values are summarized in the Table II. As one can inspect the most accurate solution is generally that based on Müller formulation, as already observed in Sect. V-A. The same result could be verified for dielectric spheres coated with a dielectric substrate, as that shown in Fig. 1 c).

For geometries as those shown in Fig. 1 e), when both hemispheres are made of the same dielectric material, numerical results are compared with those obtained for homogeneous sphere by Mie-series [13]. Table 3 shows E_{MR} obtained by EFIE, MFIE, CFIE, PMCHWT, Müller EMFIE and MEFIE formulations in this analysis. Different radius and ϵ_r values were considered. It can be observed that

TABLE II - MEAN RELATIVE ERROR (E_{MR}) FOR PEC COATED SPHERES

Sphere Radius (λ_0)		ϵ_r	E_{MR} (%)						
a	b		Müller	PMCHWT	EFIE	MFIE	CFIE	EMFIE	MEFIE
0.5	0.55	2	0.59	1.29	0.75	1.1	1.15	0.92	1.41
		4	0.93	1.18	0.97	1.34	1.22	1.09	1.12
		10	0.59	0.85	0.56	0.85	0.49	0.56	0.58
		25	0.99	14.07	0.62	0.56	0.77	0.76	0.49
		50	1.1	4.36	2.31	1.7	1.29	1.07	2.06
2	2.02	2	0.86	1.88	1.28	1.82	2.18	0.86	2.0
		4	0.94	14.48	10.59	1.84	2.63	1.22	1.31
		10	1.54	1.15	1.23	4.43	4.27	1.59	1.48
		25	0.51	0.94	0.68	0.89	1.93	0.49	0.82
		50	0.58	1.73	1.03	1.11	1.26	0.7	1.29
5	5.5	2	0.92	1.82	1.18	1.81	1.58	1.34	1.64
		4	1.2	13.63	18.06	3.02	3.13	1.81	2.82
		10	0.48	1.28	1.51	0.35	0.66	0.44	1.25
		25	0.52	0.94	0.68	0.88	1.93	0.49	0.82
		50	1.85	2.89	5.37	1.6	7.08	1.94	2.79
10	11	2	1.35	2.03	1.41	2.16	1.62	1.52	1.76
		4	1.81	7.68	6.70	7.37	6.79	5.84	8.47
		10	3.15	3.15	3.15	3.15	3.15	3.15	3.15
		25	1.24	1.24	1.24	1.24	1.24	1.24	1.24
0.5	1	2	0.73	1.15	0.79	1.1	0.93	1.00	2.68
		4	1.05	1.39	1.20	1.4	1.44	1.37	1.67
		10	0.46	1.21	1.22	2.76	0.58	0.44	0.83
		20	0.27	0.74	0.34	0.39	0.29	0.25	0.55
1	2	2	0.95	33.36	24.30	2.8	2.34	1.18	1.78
		4	0.73	4.96	0.80	1.22	7.96	0.92	2.32
		10	4.55	3.23	4.81	2.89	4.43	2.23	1.88
		20	0.14	1.41	0.24	0.37	0.34	0.2	0.38
2.5	5	2	1.09	2.26	1.75	1.36	1.23	1.05	1.64
		4	0.85	1.37	1.24	1.12	1.20	1.02	1.11
		10	0.65	1.49	1.21	0.79	1.07	0.86	31.78
		20	0.76	1.61	1.18	1.16	5.57	0.7	2.81
5	10	2	1.62	4.33	3.13	1.92	3.58	1.81	1.98
		4	1.11	1.56	2.04	2.01	2.26	1.73	2.32
		10	2.02	4.9	3.19	5.46	4.63	3.23	5.28
		20	0.95	1.36	1.09	1.43	1.15	1.06	1.45

the most accurate formulation is PMCHWT, as already observed in Sect. V-A and in [10], [14] and [15].

For all BOR analyzed in this section the computational efforts required by EFIE, MFIE, CFIE, PMCHWT, Müller EMFIE and MEFIE formulations are practically equal. For more complex geometries (coated and bisected spheres) EFIE, MFIE, EMFIE and MEFIE formulations should present smaller computational effort for z matrix evaluation, but for this type of BOR the most accurate formulations are PMCHWT and Müller for dielectric surfaces. In this work PMCHWT and Müller formulations are utilized for analysis of BOR composed of different homogeneous regions and layered BOR, respectively.

TABLE III - MEAN RELATIVE ERROR (E_{MR}) FOR BIASECTED DIELECTRIC SPHERES

Sphere radius	ϵ_{r1}	ϵ_{r2}	E_{MR} (%)						
			Müller ($\times 10^3$)	PMCHWT	EFIE ($\times 10^5$)	MFIE ($\times 10^5$)	CFIE ($\times 10^5$)	EMFIE ($\times 10^3$)	MEFIE
$0.5 \lambda_0$	4	4	0.8941	1.9682	0.0052	0.0398	0.00019	0.0772	0.0857
	10	10	0.5438	1.8529	0.0283	0.0359	0.00047	0.0162	0.0150
	20	20	6.1370	3.7427	0.0034	0.0199	0.00016	0.0351	0.0666
$2 \lambda_0$	4	4	0.0219	0.9919	0.0065	0.0212	0.00002	0.0026	0.0033
	10	10	0.1616	1.2222	0.0102	0.1162	0.00038	0.0264	0.0288
	20	20	0.3574	4.0820	0.0138	0.2778	0.00092	0.0057	0.0043
$5 \lambda_0$	4	4	0.0125	0.6976	0.0084	0.0150	0.00001	0.0009	0.0010
	10	10	0.0803	5.0943	0.0711	0.3470	0.00249	0.0070	0.0264
	20	20	0.0922	3.2636	0.0661	0.1881	0.00012	0.0074	0.0174
$10 \lambda_0$	4	4	0.0079	0.4653	0.0128	0.0194	0.00001	0.0006	0.0007
	10	10	0.0431	1.5493	0.2334	0.2581	0.00014	0.0023	0.0018
	20	20	0.1378	9.8286	0.4199	0.8245	0.00095	0.0119	0.0190
$20 \lambda_0$	4	4	0.0039	0.4850	0.0167	0.0098	0.00001	0.0006	0.0012
	10	10	0.0207	3.3251	0.0206	0.0820	0.00007	0.0045	0.0116
	20	20	0.1378	9.8286	0.4199	0.8245	0.00095	0.0119	0.0190

VI. OPTIMUM NUMBER OF BASIS FUNCTIONS

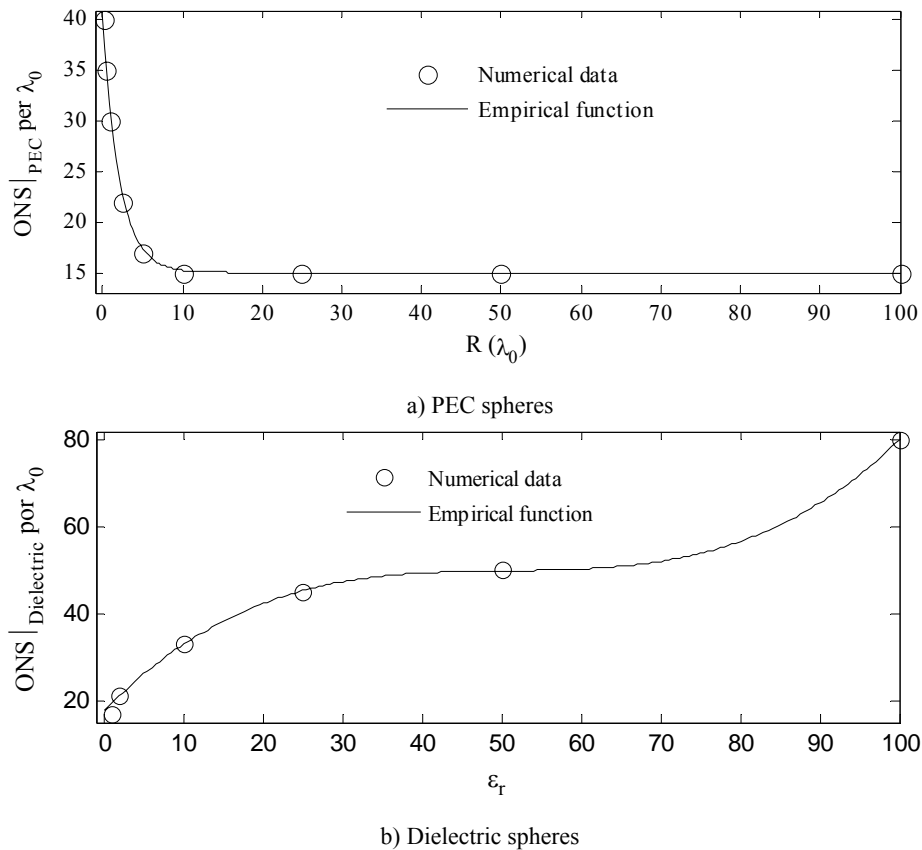
To obtain the optimum number of segments per λ_0 (i.e., basis functions), ONS per λ_0 , the plane-wave scattering by PEC, dielectric and composite spheres was analyzed for several different ϵ_r and sphere electrical radii ($R(\lambda_0)$). For each computation, the ONS was attained for E_{MR} error smaller than 1.0 %, with respect to the Mie series solutions [13]. The analysis was performed using CFIE formulation for PEC surfaces and Müller/PMCWHT formulations for dielectrics ones. Fig. 12 a) shows the ONS per λ_0 for PEC spheres as function of $R(\lambda_0)$ and Fig. 12 b) shows the ONS per λ_0 for dielectric spheres, which radius R_D varying from $0,5 \lambda_0$ to $75 \lambda_0$, as function of ϵ_r . For PEC spheres it can be observed that as $R(\lambda_0)$ increases (i.e., as the sphere curvature diminishes), less segments per λ_0 are needed. For dielectric spheres it can be observed that the variation of ONS per λ_0 with the increase of $R(\lambda_0)$ is practically insignificant, but as ϵ_r increases more segments per λ_0 are needed. From the numerical data indicated in Fig. 12, empirical formulas for the ONS per λ_0 were obtained:

$$\text{ONS}|_{\text{PEC}} = 14.636 + 29.615 e^{-0.8759R}, \quad (14)$$

$$\text{ONS}|_{\text{Diélectric}} = 0.00024 \epsilon_r^3 - 0.036 \epsilon_r^2 + 1.87 \epsilon_r + 17.71, \quad (15)$$

which provide the curves illustrated in Fig. 12.

For composed spheres as that shown in Fig. 1 b) to e) conducting surface should be analyzed by CFIE formulation with number of segments determined by (14) and for dielectric surfaces Müller and PMCWHT formulations should be used for layered dielectric bodies and bodies composed of different homogeneous regions, respectively, with number of segments determined by (15).

Fig. 12. ONS per λ_0 .

VII. PRACTICAL CASE

In this Section empirical formulas obtained in Section VI were used to obtain the optimum number of segments per λ_0 to analyze of omnidirectional double reflector antennas. For antenna shown in Fig. 13, which is excited by the fundamental mode TEM, the gain obtained employing 70%, 100% and 130% of segments indicated by (15) are shown in Fig. 14. The comparison between the results obtained employing 100% and 130% of segments and that available in [16] demonstrate a very good agreement between solutions, what indicate that it is employed enough number of segments to attain desired accuracy. However, when it is used 70% of segments the radiation pattern is slightly modified (i.e., the main lobe suffers a little alteration, but secondary lobes are significantly altered). In this analysis conducting open and closed surfaces were evaluated by EFIE and CFIE, respectively.

Considering the same omnidirectional double reflector antenna, but now with a dielectric radome with relative permittivity $\epsilon_r = 2.08$, as that illustrated in Fig. 15, where λ_d is the wavelength of dielectric radome, the gain obtained is shown in Fig. 16. The number of segments for conducting and dielectric surfaces was defined conform (14) and (15), respectively. Dielectric and conducting surfaces were analyzed by PMCWHT and CFIE formulations, respectively. For dielectric surfaces other formulations (EFIE, MFIE, CFIE, Müller, EMFIE and MEFIE) do not generated good results, as

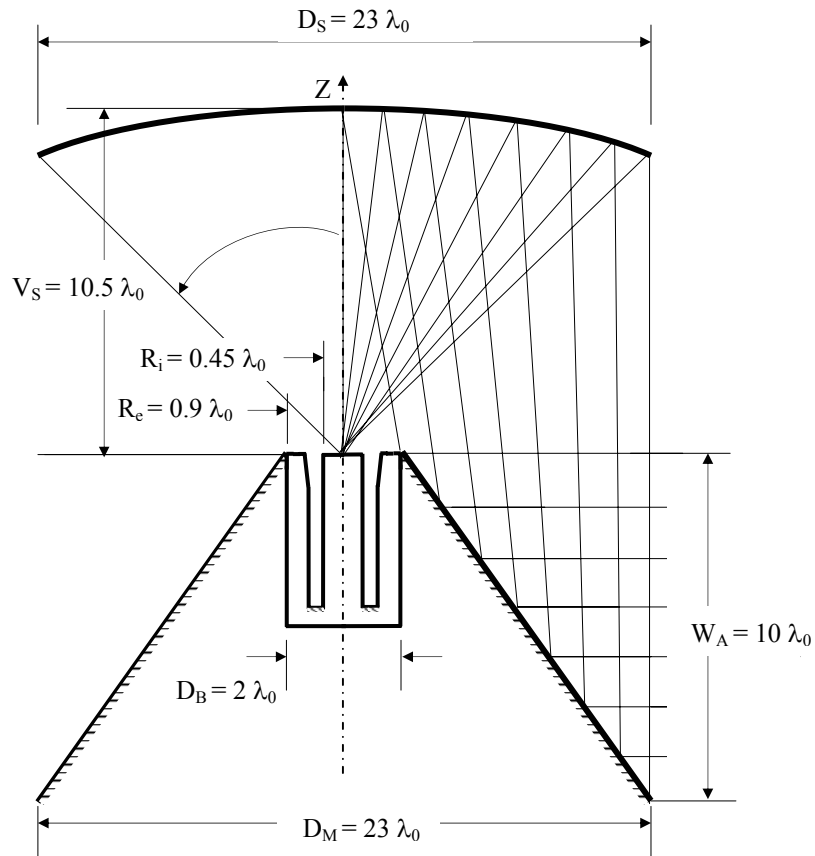


Fig. 13. Double reflector omnidirectional antenna.

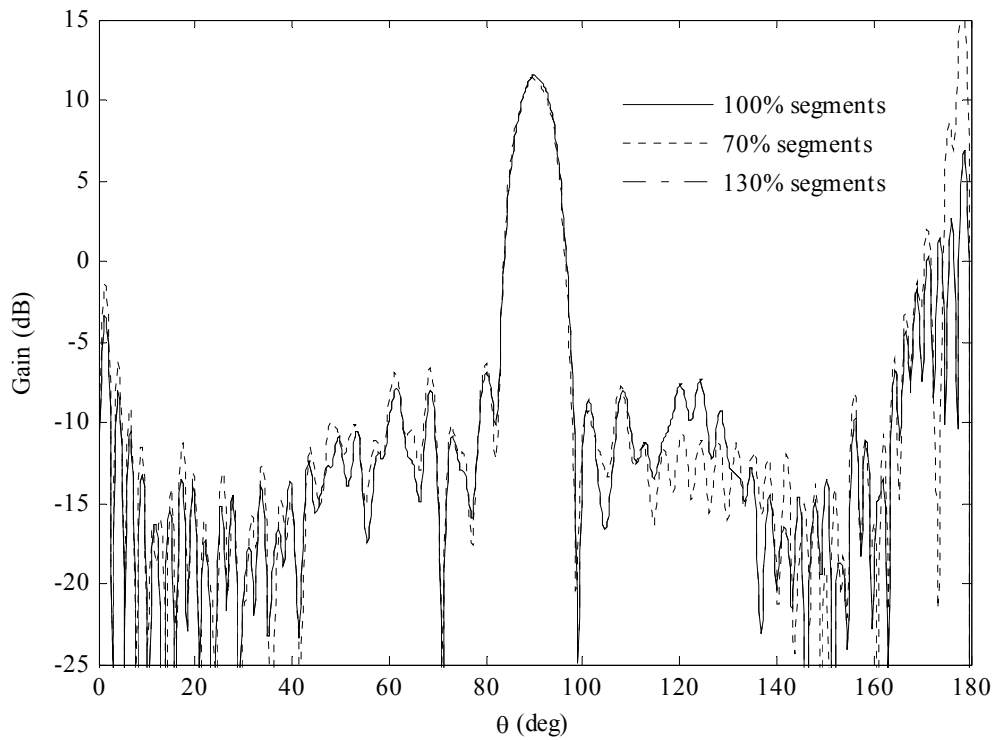


Fig. 14. Radiation pattern for double reflector omnidirectional antenna.

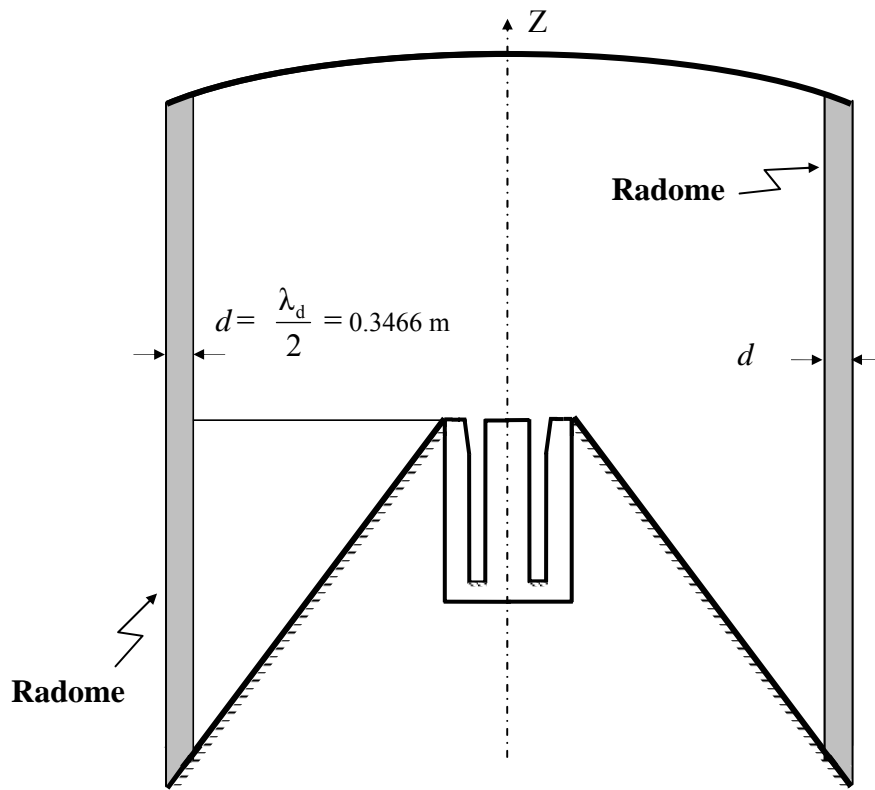


Fig. 15. Double reflector omnidirectional antenna with radome.

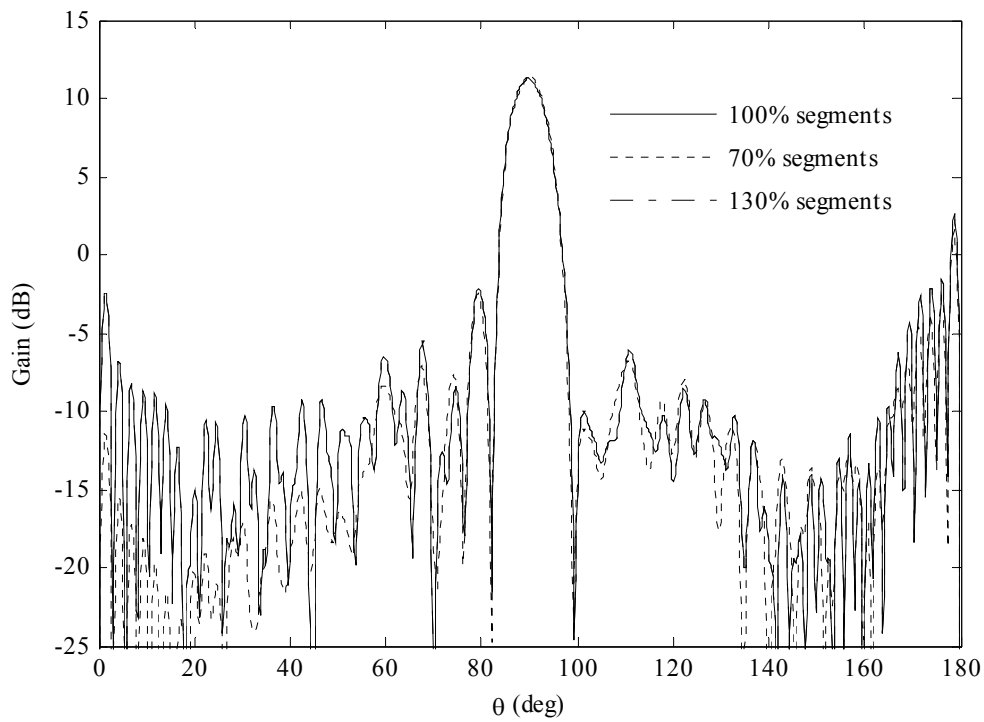


Fig. 16. Radiation pattern for double reflector omnidirectional antenna with radome.

indicated in Section V for BOR constituted of different regions and in [10], [15] and [15]. It can be verified that the radome do not alter significantly de antenna electromagnetic behavior, and the same results were found when the number of segments is altered (i.e., when are employed 130% of segments the results do not presents any alteration, but when are employed 70% of segments are used pattern is modified, the main lobe suffer a little alteration, but secondary lobes are significantly altered).

The Table 4 shows the maximum gain obtained in the all analysis of omnidirectional double reflector antenna. It can be verified that when 100% and 130% of segments are employed the maximum is not modified.

TABLE IV – MAXIMUM GAIN FOR OMNIDIRECTIONAL ANTENNA

Gain (dB)					
Ominidirectional double reflector antenna			Ominidirectional double reflector antenna with radome		
70 % segments	100 % segments	130 % segments	70 % segments	100 % segments	130 % segments
16.14 (secondary lobe)	11.52 (main lobe)	11.55 (main lobe)	11.4735 (main lobe)	11.28 (main lobe)	11.31 (main lobe)

VIII. CONCLUSIONS

In the present work we presented and investigate two new formulations for solution of the electromagnetic scattering by dielectric and composite bodies of revolution. The equivalent current representation adopted is the versatile triangular basis functions for \hat{t}' and $\hat{\Phi}'$ directions. The new formulations accuracy was analyzed by the plane-wave scattering from dielectric and composite spheres of different electrical sizes and different relative permittivity values. The test results indicated that, in the most of cases, the new formulations accuracy is slightly smaller than classical formulations, Müller and PMCHWT, accuracy and that EMFIE formulation seems to be better than MEFIE.

The electromagnetic scattering from dielectric and composed spheres at different sizes was analyzed using different integral-equation formulations. Spheres with radii varying from 0.5 up to 25 free-space wavelengths were considered. The dielectric relative permittivity was varied from 1 to 100. It was verified that Müller integral equation may provide the most accurate solutions for homogeneous and layered dielectric bodies, and PMCWHT integral equation may provide the most accurate solutions for bodies composed of different homogeneous regions, independently of the radii and relative permittivities values. It was also verified that, for geometries evaluated in this work, the computational efforts required by EFIE, MFIE, CFIE, PMCHWT, Müller EMFIE and MEFIE formulations are practically equal.

Closed conducting and dielectric surfaces were analyzed by CFIE and Müller (PMCWHT) formulation, respectively. Then, for several different dielectric, conducting and composite spheres, we obtained the minimum number of segments (i.e., basis functions) necessary to attain a desired accuracy for the current representation. The study leded to empirical formulas that provide the

optimal (minimum) number of segments (ONS) in terms of the sphere relative permittivity (for dielectrics) and electrical radius. Such formulas were used in the choice of the number of basis functions for omnidirectional double-reflector antenna analysis and it was demonstrated that such empirical formulas are able to provide the necessary ONS for analysis of more complex BOR.

REFERENCES

- [1] S. M. Rao, C. C. Cha, R. L. Cravey, and D. Wilkes, "Electromagnetic scattering from arbitrary shaped conducting bodies coated with lossy materials of arbitrary thickness," *IEEE Trans. Antennas Propagat.*, vol. 39, pp. 627–631, May 1991.
- [2] S. M. Rao, T. K. Sarkar, P. Midya, and A. R. Djordjevic, "Electromagnetic radiation and scattering from finite conducting and dielectric structures: Surface/surface formulation," *IEEE Trans. Antennas Propagat.*, vol. 39, pp. 1034–1037, July 1991.
- [3] A. W. Glisson, "On the development of numerical techniques for treating arbitrarily-shaped surfaces," Ph.D. Dissertation, University of Mississippi, June 1975.
- [4] J. R. Mautz and R. F. Harrington, "An improved E-Field solution for a conducting body of revolution," Tech. Report TR-80-1, Dept. Electrical and Computer Engineering, Syracuse University, 1980.
- [5] J. R. Mautz and R. F. Harrington, "H-Field, E-Field and combined field solutions for bodies of revolution," Tech. Report TR-77-2, Dept. Electrical Computer Engineering, Syracuse University, 1977.
- [6] J. R. Mautz and R. F. Harrington, "Electromagnetic scattering from a homogeneous body of revolution," Tech. Report TR-77-10, Dept. Electrical and Computer Engineering, Syracuse University, 1977.
- [7] P. Ylä-Oijala and M. Taskinen, "Well-conditioned Müller formulation for electromagnetic scattering by dielectric objects," *IEEE Trans. Antennas and Propagation*, vol. 53, no. 10, pp. 3316–3323, Oct. 2005.
- [8] A. A. Kishk, L. Shafai, "Different formulations for numerical solutions of single or multibodies of revolution with mixed boundary conditions," *IEEE Trans. Antennas and Propagation*, vol. 34, no. 5, pp. 666–673, May 1986.
- [9] A. A. Kishk, L. Shafai, "Numerical solutions of scattering from coated bodies of revolution using different integral equation formulations," *IEE Proceedings*, vol. 133, Pt. H, no. 3, pp. 227–231, Jun 1986.
- [10] P. L. Huddleston, L. N. Medgyesi-Mitschang and J. M. Putnam, "Combined field integral equation formulation for scattering by dielectrically coated conducting bodies," *IEEE Antennas and Propagation*, vol. 34, no. 4, pp. 510–520, April 1986.
- [11] L. N. Medgyesi-Mitschang and J. M. Putman, "Electromagnetic scattering from axially inhomogeneous bodies of revolution," *IEEE Trans. Antennas and Propagation*, vol. 32, no. 8, pp. 797–806, August 1984.
- [12] Y. Chu, W. C. Chew, J. Zhao, S. Chen, "A surface integral equation formulation for low-frequency scattering from a composite object," *IEEE Trans. Antennas Propagat.*, vol. 51, no. 10, pp. 2837–2844, October 2003.
- [13] G. Mie, "Beitrage zur optik trüber medien, speziell kolloider metallo-sungen," *Ann. Phys.*, vol. 25, p. 377, 1908
- [14] Y. Chu, W. C. Chew, S. Chen and J. Zhao, "Generalized PMCHWT formulation for low-frequency multi-region problems," *Proc. IEEE AP-S Symp.*, vol. 3, 2002, pp. 664–667.
- [15] Y. Chu, W. C. Chew, J. Zhao and S. Chen, "A surface integral equation formulation for low-frequency scattering from a composite object", *IEEE Transactions on Antennas and Propagation*, AP-51, No. 10, pp. 2837–2844, October 2003.
- [16] F. J. S. Moreira, A. Prata, Jr. and J. R. Bergmann, "GO Shaping of Omnidirectional Dual-reflector Antennas for a Prescribed Equi-Phase aperture Field Distribution", *IEEE Antennas and Propagation*, vol. 55, no. 1, pp. 99–106, January 2007.